4.3 Cape Cod Study

The case study presented in Appendix 1 was adapted from USGS open file reports 84-475 and 86-481 (de Lima and Olimpio, 1984 and Ragone, 1986 respectively). The study was conducted at Cape Cod, Massachusetts in the United States of America. Treated sewage had been discharged through infiltration beds into underlying sand and gravel aquifer since 1936 at an approximate rate of 0.46 Mgal/day. The contaminant plume that resulted from the discharge was estimated to be 11000 ft long, 3000 ft wide and 75 ft thick. The geology of the area consists of glacial deposits that are underlain by crystalline bedrock. The uppermost 90 to 140 ft consists of stratified sand and gravel which overlies silty sand and till. Average hydraulic conductivity of the aquifer materials was determined to be 380 ft/day and the average linear groundwater velocity was estimated as 1.5 ft/day. A numerical model was developed to provide insight to hydraulic processes at the site and predict the response of the system to different hydraulic stresses. Appendix 1 presents site characterization in cross section and plan view, conceptualization of the problem domain in terms of boundary conditions, discretization of the problem domain, and comparison of results of the calibrated model with the observed data.

5. FINITE ELEMENTS

5.1 Basic Principles

The main advantage of the finite element method is that domains of irregular geometry can be represented naturally. This advantage comes into play with 2D and 3D problems. Thus, although finite element solutions can be developed for any dimensionality, we will focus here on 2D domains. Regardless of the spatial dimensionality, the time dimension always has the same uniformity and is therefore usually handled with finite differences, even when the spatial dimensions are handled with finite elements. Comprehensive discussions of the finite element

method in groundwater hydrology may be found in texts such as Huyakorn and Pinder (1983).

In applying the finite element method, we start by dividing the domain into a number of elements (Fig. 16). Many element shapes are possible; in two dimensions, the most useful shape for groundwater problems is the linear triangle. The points where the element corners meet are the *nodes*.

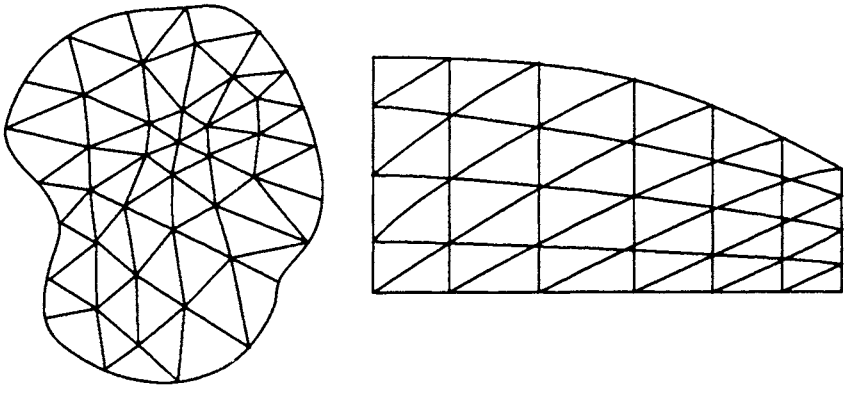

Figure 16: Typical finite element grids

The first step in the development of the finite element solution is to define an *interpolation function* that expresses the value of the unknown function u=u(x,y) in terms of its values u_j at the nodes (Fig. 17). The interpolation is accomplished by means of *basis functions*. For the linear triangle, these basis functions are inclined planes of the form shown in Fig. 18. There is one basis function for each of the 3 nodes on the element; each of these basis functions has a value of 1 at the node it represents, and a value of 0 at the other two nodes that lie on the same element.

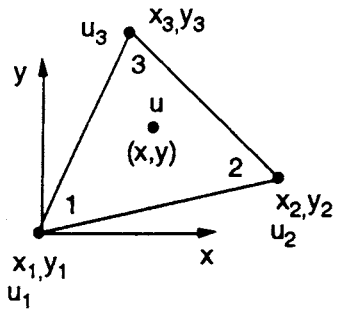

Figure 17: Typical linear triangle element

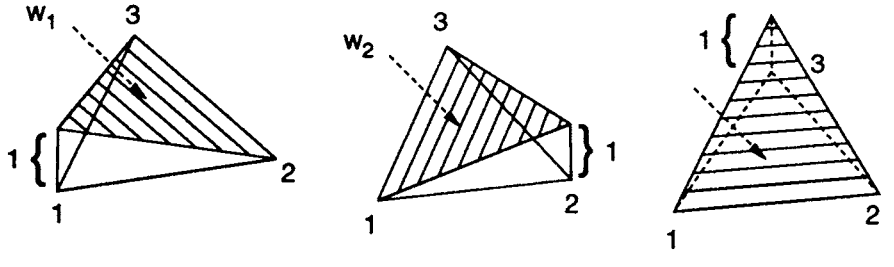

Figure 18: Basis functions for linear triangle

Since the basis functions are linear, the interpolation will be a piecewise linear approximation of u. We call the approximate function $\hat{u}=\hat{u}(x,y)$. The interpolation that expresses $\hat{u}$ in terms of u_j is:

$$\hat{u}(x,y) = \sum_{j=1}^{3} u_j w_j(x,y)$$

where $w_j(x,y)$ represents the basis functions. For the linear triangle, these are surfaces given by:

$$w_j(x,y) = \frac{1}{2\Delta}(a_j + b_j x + c_j y)$$

where the coefficients are obtained by cyclic permutation of the nodes i,j,k as follows (Zienkiewicz, 1977):

$$a_i = x_j y_k - x_k y_j$$

$$b_i = y_j - y_k$$

$$c_i = x_k - x_j$$

and where the determinant is defined as:

$$\det = 2\Delta = \begin{bmatrix} 1 & x_i & y_i \\ 1 & x_j & y_j \\ 1 & x_k & y_k \end{bmatrix}$$

with Δ being the area of the triangle. A property of the basis functions is that:

$$\sum_{j=1}^{3} w_j(x,y) = 1$$

everywhere within the element.

The second step in developing the finite element solution is the generation of the algebraic equations that will be solved for the unknown nodal values. To generate these equations, we use the *Weighted Residual Method* (Huyakorn and Pinder, 1983). Suppose we have a partial

differential equation of the form:

$$L(u) - f = 0$$

where L is a differential operator. An exact solution will be obtained if we substitute a trial solution in the form of:

$$u(x,y) = \lim_{n\to\infty} \sum_{j=1}^{n} u_j w_j(x,y)$$

where n is the number of nodes in the domain. If we limit the nodes to a finite number, as we must, the solution will be approximate and of the form:

$$u(x,y) \approx \hat{u}(x,y) = \sum_{j=1}^{n} u_j w_j(x,y)$$

where $\hat{u}$ designates an approximation of u. We can substitute the approximate solution into the original differential equation to obtain:

$$L(\hat{u}(x,y)) - f = R(x,y) \neq 0$$

where the non-zero residual function R(x,y) on the right-hand side is a consequence of the approximation.

According to the theory of weighted residuals, we can minimize the residual R(x,y) on the average over the domain by satisfying a set of weighted residual equations, which are:

$$\int_A R(x,y)\ w_i(x,y)dA = 0 \qquad i=1,2,\cdots,n$$

where A designates the solution domain, and $w_i(x,y)$ are a set of n weighting functions corresponding to the nodes (Fig. 19).

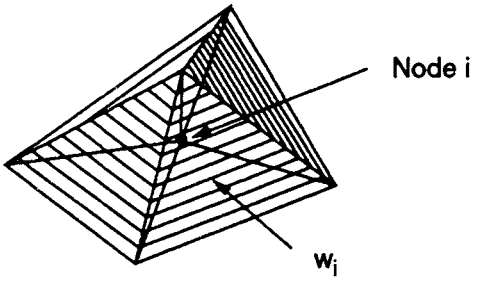

Figure 19: Linear weighting function

In the general weighted residual method, these *weighting functions* are independently chosen. In the *Galerkin Method*, on the other hand, which is a special variant of the weighted residual method, the weighting functions are chosen to be identical to the basis functions. This has the advantage of simplicity, and a further advantage in that the coefficient matrix for the flow equation becomes symmetrical. The Galerkin Method has been well proven in groundwater hydrology (Pinder and Frind, 1972) and we will here use it exclusively.

The numerical error in the Galerkin finite element method is *minimized globally*; that is, over the domain as a whole, the error is a minimum. As the number of nodes increases and the nodal distances decrease, the error decreases, and, in the limit as the number of nodes tends to infinity, the error tends to zero. Locally, the numerical error is of first order for non-uniform node spacing and of second order for uniform node spacing.

5.2 Finite Element Solution of 2D Flow Equation

The governing equation for flow in a heterogeneous isotropic medium, with the coordinate axes oriented along the principal directions of conductivity, is:

$$\frac{\partial}{\partial x}\left(K_{xx}\frac{\partial u}{\partial x}\right) + \frac{\partial}{\partial y}\left(K_{yy}\frac{\partial u}{\partial y}\right) - S_s\frac{\partial u}{\partial t} = 0$$

where u is the unknown potential. The boundary and initial conditions are of the form:

$$u=u_c \qquad on\ B_1 \quad (first\text{-}type)$$

$$-K_n\frac{\partial u}{\partial n} = q_n \quad on\ B_2 \quad (second\text{-}type)$$

$$u=u_0 \qquad at\ t=t_0$$

where B_1 and B_2 are parts of the boundary with $B = B_1 + B_2$ being the complete domain boundary, K_n is the effective hydraulic conductivity in the direction of the normal at the boundary, and t_0 is the initial time.

To develop the Galerkin finite element solution, we discretize the spatial domain with linear triangular elements and assume a trial solution of the form:

$$u(x,y) \approx \hat{u}(x,y) = \sum_{j=1}^{n} u_j w_j(x,y)$$

Upon substitution of the trial solution into the governing equation, a residual will be obtained which is:

$$R(x,y) = \frac{\partial}{\partial x}\left(K_{xx}\frac{\partial \hat{u}}{\partial x}\right) + \frac{\partial}{\partial y}\left(K_{yy}\frac{\partial \hat{u}}{\partial y}\right) - S_s\frac{\partial \hat{u}}{\partial t}$$

According to weighted residual theory, the residual will be minimized if a set of weighted residual equations is satisfied. The weighted residual will be minimized if a set of weighted residual equations is satisfied. The weighted residual equations are of the general form:

$$\int_A R(x,y)\ w_i(x,y)\ dxdy = 0 \qquad i = 1\ ,\ 2\ ,\ \cdots\ ,\ n$$

or specifically, for the case of the 2D flow equation:

$$\int_A \left\{ \frac{\partial}{\partial x}\left(K_{xx}\frac{\partial \hat{u}}{\partial x}\right) + \frac{\partial}{\partial y}\left(K_{yy}\frac{\partial \hat{u}}{\partial y}\right) - S_s\frac{\partial \hat{u}}{\partial t} \right\} w_i(x,y)\ dxdy = 0 \qquad i=1,2,\ \cdots\ ,\ n$$

The approximate functions u in the above equation are represented within each element by the interpolation function:

$$\hat{u}(x,y) = \sum_{j=1}^{3} u_j\ w_j(x,y)$$

which expresses $\hat{u}$ in terms of the unknown nodal values u_j.

The Galerkin procedure calls for the interpolation function to be substituted into the weighted residual equations. We note that, since the interpolation function is expressed in terms of the linear basis functions $w_j(x,y)$, evaluation of the second derivatives in the weighted residual equations will cause the equations to vanish. To overcome this problem, we first transform the second-derivative terms by applying Green's theorem (Hildebrand, 1965). The result is:

$$\int_A \left\{ K_{xx}\frac{\partial w_i}{\partial x}\frac{\partial \hat{u}}{\partial x} + K_{yy}\frac{\partial w_i}{\partial y}\frac{\partial \hat{u}}{\partial y} \right\} dxdy$$

$$+ \int_B \left\{ K_{xx}\frac{\partial \hat{u}}{\partial x}\ l_x + K_{yy}\frac{\partial \hat{u}}{\partial y}\ l_y \right\} w_i(x,y)\ db$$

$$+ \int_A S_s \frac{\partial \hat{u}}{\partial t} w_i(x,y)\, dxdy = 0 \qquad i=1,2, \cdots, n$$

where l_x, l_y are the direction cosines of the inward normal at the boundary, and db is an increment of the boundary. The inward rather than the outward normal is chosen in order to be consistent with the mass conservation convention which specifies that mass added to the system is positive.

We can now substitute the interpolation function for the variable u. The nodal values u_j contained in the interpolation function, being point values, can be taken outside the integral. Also, since the basis functions, which must be integrated, are defined individually for the elements, we can break up the entire integral into elemental contributions which are summed over all the elements. Furthermore, the boundary integral in the above equation represents the second-type (flux) boundary condition $q_n=-K_n\partial u/\partial n$, which allows us to replace the term {.} by the boundary flux $\{-q_n\}$. The boundary integral is known as the *natural boundary condition* since it is generated naturally by the weighted residual finite element formulation.

Finally, we let the time derivative be approximated by:

$$\frac{\partial \hat{u}}{\partial t} = \frac{\partial}{\partial t}\left(\sum_{j=1}^{n} u_j w_j(x,y)\right)$$

The weighted residual equations thus become:

$$\sum_{j=1}^{n} u_j \sum_{e} \int_{A^e} \left\{ K_{xx} \frac{\partial w_i}{\partial x} \frac{\partial w_j}{\partial x} + K_{yy} \frac{\partial w_i}{\partial y} \frac{\partial u_j}{\partial y} \right\} dxdy$$

$$- \sum_{e} \int_{B^e} q_n w_i db + \sum_{j=1}^{n} \frac{\partial u_j}{\partial t} \sum_{e} \int_{A^e} S_s \, w_i w_j \, dxdy = 0 \qquad i=1,2, \cdots, n$$

where A^e represents the element area, and B^e represents the side of an element lying on the boundary. The above n equations can be written in summation notation as:

$$\sum_{j=1}^{n} u_j M_{ij}^{K} + \sum_{j=1}^{n} \frac{\partial u_j}{\partial t} M_{ij}^{S} - F_i^{B} = 0 \qquad i=1,2, \cdots, n$$

or in matrix notation as:

$$[M^K]\{u\} + [M^S] \left\{ \frac{\partial u}{\partial t} \right\} - \{F^B\} = 0$$

where $[M^K]$ is the conductance matrix, $[M^S]$ is the storage matrix, and $\{F^B\}$ is the boundary flux vector. The coefficient matrices are now entirely in terms of material parameters and geometric terms which express the element geometry through the basis functions. The procedure for evaluation of the matrices is to first generate the elemental coefficient matrices and then to assemble these into the corresponding global matrices. The elemental matrices corresponding to the specialized equations addressed here are given in Sections 5.4, 5.5, and 5.6.

The time derivative can be approximated by a forward difference approximation of the form:

$$\frac{\partial u}{\partial t} = \frac{u_{k+1} - u_k}{\Delta t}$$

where k designates the time level. In order to obtain optimum accuracy and unconditional stability, we can place the spatial terms in the equation at a point in time where the time derivative approximation has the lowest error. In most cases this is the midpoint between the old and the new time levels, or $t_k + \Delta t/2$ (centered difference approximation). However, we can also choose a general time weighting of the form $t_k + \eta\Delta t$, where $0 \leq \eta \leq 1$. The spatial

terms will then be weighted in time according to:

$$\eta\ u_{k+1} + (1-\eta)u_k$$

On the basis of a general time weighting, the matrix equation becomes:

$$\left\{ \eta[M^K] + \frac{1}{\Delta t}[M^S] \right\} \{ u \}_{k+1} = \left\{ -(1-\eta)[M^K] + \frac{1}{\Delta t}[M^S] \right\} \{ u \}_k + \eta\{ F^B \}_{k+1} + (1-\eta)\{F^B\}_k$$

where $\eta = 1$ gives an implicit-in-time solution and $\Delta=1/2$ gives a centered-in-time solution.

To account for the first-type boundary condition, the matrix equation is partitioned according to nodes at which u is unknown and nodes at which u is known. The partitioning is as follows:

$$\left[\begin{array}{c|c} M_{ff} & M_{fc} \\ \hline M_{cf} & M_{cc} \end{array}\right] \left\{\begin{array}{c} u_f \\ \hline u_c \end{array}\right\} = \left\{\begin{array}{c} F_f \\ \hline F_c \end{array}\right\}$$

where M and F stand for the complete coefficient matrix (left-hand side) and forcing vector (right-hand side) of the finite element matrix equation, respectively, and where the subscripts f and c designate free nodes (u unknown) and constrained nodes (u specified), respectively.

The partitioned equation is multiplied out to give:

$$[M_{ff}] \{ u_f \} + [M_{fc}] \{ uc \} = \{ F_f \}$$

$$[M_{cf}] \{ u_f \} + [M_{cc}] \{ u_c \} = \{ F_c \}$$

Only the first of these two equations is needed for the solution. The second equation is used if the fluxes at the first-type boundary are required, for example, in mass balance calculations. The second term in the first equation, which represents the link between the first-type boundary nodes and the interior nodes of the domain, contains known terms only and is moved to the right-hand side. The equation to be solved thus becomes:

$$[M_{ff}] \{ u_f \} = \{ F_f \} - [M_{fc}] \{ u_c \}$$

where the right-hand side now contains all known quantities, which include the solution at the preceding time step, values at the first-type boundary, and fluxes at the second-type boundary.

The above matrix equation, which is typical for flow problems and purely diffusive problems, has symmetric coefficient matrices. The usual method of solution is the Cholesky method, which takes advantage of matrix symmetry. For the 1D form, the Thomas method is commonly used. For very large systems, the preconditioned conjugate gradient method (Schmid and Braess, 1988) is now becoming increasingly popular.

After solution of the matrix equations, the specific discharge in each element can be calculated by substituting the potentials into the Darcy equation (Section 2.1). The elemental interpolation function is used to express the potential function in term of the nodal values u_j produced by the matrix solution. For the case where the coordinate axes coincide with the principal directions of conductivity, the components of specific discharge in 2D become:

$$q_x = -\frac{K_{xx}}{2\Delta} \sum_{j=1}^{3} u_j b_j$$

$$q_y = -\frac{K_{yy}}{2\Delta} \sum_{j=1}^{3} u_j c_j$$

where b_j,c_j are the basis function coefficients. The groundwater velocities are then given by $v_i=q_i/\theta$. Since the basis function coefficients, which result from the differentiation of the linear basis function, are constant over each element, the velocity components will be element-wise constant, and discontinuous from one element to the next.

Matrix equations similar to the above can be developed for the various specialized equations for flow and transport. The finite element solutions for the three types of equations given in Section 2 are developed below.

5.3 Anisotropy and Heterogeneity

The above development is valid for isotropic material or anisotropic material with the coordinate axis coinciding with the principal directions of anisotropy. For the more general case, where the coordinate axes do not coincide with the principal directions (Fig. 20), we can choose one of two options. The first is to include the cross-derivative terms in the development of the solution. The second option is to rotate the coordinate axes into the principal directions. The second option is computationally more efficient, since the terms in the finite element equation are kept to a minimum. This option should be used where the principal directions are invariant, and where the rotation is easily accomplished, as for example in 2D flow problems.

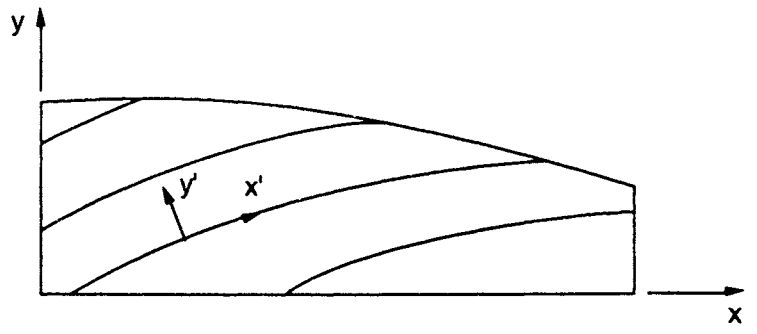

Figure 20: General anisotropic

The rotation is performed on the nodal coordinates on a node-by-node basis, according to (Fig. 21):

$$\begin{Bmatrix} x' \\ y' \end{Bmatrix} = \begin{bmatrix} \cos\beta & \sin\beta \\ -\sin\beta & \cos\beta \end{bmatrix} \begin{Bmatrix} x \\ y \end{Bmatrix}$$

where x′, y′ are the coordinates of point x,y in the principal direction coordinate system, and β is the angle between the cartesian axes and the principal axes. The finite element formulation permits each element to have its own individual angle of rotation. This is a significant advantage for cross-sectional systems with complex stratification.

The calculated potentials, being scalar quantities, are independent of the rotation. However, the velocities, being vector quantities, must be rotated back to cartesian coordinates if the velocity calculation was done in rotated coordinates (see preceding section). The back rotation

is:

$$\begin{Bmatrix} v_x \\ v_y \end{Bmatrix} = \begin{bmatrix} \cos\beta & -\sin\beta \\ \sin\beta & \cos\beta \end{bmatrix} \begin{Bmatrix} v'_x \\ v'_y \end{Bmatrix}$$

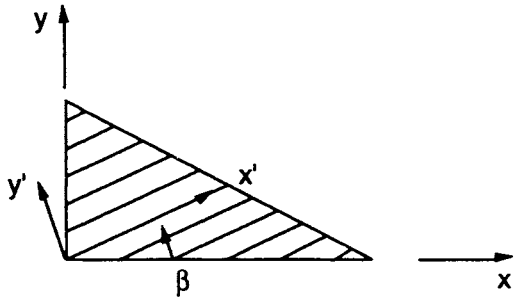

Figure 21: Rotation of axes

The problem of anisotropy also arises in the solution of the transport equation (Section 5.6). In this case, the principal directions are the directions parallel and perpendicular to the flow. Unfortunately, these directions are in general not invariant, since they depend on the flow boundary conditions. The standard procedure in transport modelling is, therefore, to use cartesian coordinates and to include the cross-derivative terms. One conceptual dilemma in this approach is that the cross derivative terms in the dispersion tensor ($D_{xy'}$ D_{yx}) are usually defined according to the classical approach, which is now recognized to be valid only at the local scale. Lacking practical alternatives, however, most models also apply the classical definition to the field scale. This is defensible on the basis that the dominant direction of contaminant migration in most aquifers is horizontal.

In situations where depth-dependent chemical or biochemical reactions occur, the vertical positioning of the plume may be of importance. In such cases, the cartesian form may not

give sufficient accuracy in the solution of the transport equation. This problem can be overcome by solving the transport equation in principal coordinates (see for example Frind *et al.*, 1990). The finite element grid for the transport solution is, in that case, defined by the flownet (see Section 4.5), which is generated by the solution of the potential and streamfunction equations. In this approach, the flow velocities are not needed in the solution of the transport equation, since the advective displacement is defined by the streamfunction solution.

The finite element formulation also accommodates material heterogeneity in a unique way. Heterogeneity is reflected in the governing equations in that the material properties, i.e. K_{ij} and D_{ij}, are functions of space and are therefore included as part of the argument of the differential operator. This would normally result in terms of the form $\partial K_{ij}/\partial x_j$ or $\partial D_{ij}/\partial x$ (see Section 5.3). These terms, however, do not appear in the finite element equation. This is due to the transformation of the differential terms by Green's Theorem, resulting in a boundary integral term and an area integral term in which the material property is no longer an argument of the differential operator. The boundary integral term vanishes in the interior of the grid because the fluxes crossing the inter-element boundaries cancel each other. The end result of this is that the finite element equations are fully valid for heterogeneous systems without derivatives of the material property functions.

5.4 Confined/Unconfined Aquifer Equations

The governing equations for flow in confined or unconfined aquifers are given in Section 2.3. The basic assumptions are that flow in the aquifer is predominantly horizontal, and that the aquifer is separated from neighbouring flow systems by aquitards whose permeability is substantially lower than that of the aquifer. A confined aquifer receives recharge mainly by leakage through the aquitards from above or below, while an unconfined aquifer receives recharge through infiltration from above. In addition, both can be recharged at the lateral boundaries, or by injection.

We assume that the coordinate axes coincide with the principal directions of transmissivity. Since the flow solution is fairly insensitive with respect to the time derivative approximation, we use backward differences in time. The finite element equation for both confined and unconfined aquifers then takes the form:

$$\left([M^K] + [M^L] + \frac{1}{\Delta t}[M^S]\right)\{\phi\}_{k+1} = \frac{1}{\Delta t}[M^S]\{\phi\}_k + \{F^R\} + \{F^B\} + \{F^Q\}$$

where k is the time level, $[M^K]$ is the conductance matrix, $[M^L]$ represents the leakage flux, $[M^S]$ is the storage matrix, and $\{F^R\}$, $\{F^B\}$, $\{F^Q\}$ represent the areal recharge flux, the boundary recharge flux, and the source/sink recharge flux, respectively.

For a grid consisting of linear triangular elements, the elemental components of the above matrices are defined as follows:

$$[M^K]^e = \frac{T_{xx}}{4\Delta}\begin{bmatrix} b_1b_1 & b_1b_2 & b_1b_3 \\ b_2b_1 & b_2b_2 & b_2b_3 \\ b_3b_1 & b_3b_2 & b_3b_3 \end{bmatrix} + \frac{T_{yy}}{4\Delta}\begin{bmatrix} c_1c_1 & c_1c_2 & c_1c_3 \\ c_2c_1 & c_2c_2 & c_2c_3 \\ c_3c_1 & c_3c_2 & c_3c_3 \end{bmatrix}$$

$$[M^L]^e = \left(\frac{K'_1}{b'_1} + \frac{K'_2}{b'_2}\right)\frac{\Delta}{12}\begin{bmatrix} 2 & 1 & 1 \\ 1 & 2 & 1 \\ 1 & 1 & 2 \end{bmatrix}$$

$$[M^S]^e = \frac{\Delta}{12}\begin{bmatrix} 2 & 1 & 1 \\ 1 & 2 & 1 \\ 1 & 1 & 2 \end{bmatrix}$$

$$\{F^R\}^e = \left(\frac{K'_1}{b'_1}h_1 + \frac{K'_2}{b'_2}h_2 + q_R\right)\frac{\Delta}{3}\begin{Bmatrix}1\\1\\1\end{Bmatrix}$$

$$\{F^B\}^e = q_n\frac{L^e}{2}\begin{Bmatrix}1\\1\end{Bmatrix}$$

where b_j, c_j are the basis function coefficients, Δ is the element area, K'_1, K'_2, b'_1, b'_2 represent the hydraulic conductivity and thickness of the upper and lower aquitards, respectively; h_1, h_2 are the heads in the adjoining aquifers that contribute leakage flux; q_R is the recharge at the watertable; q_n is the influx at the lateral (second-type) boundaries, and L^e is the length of the elements at the boundary. The source/sink vector $\{F^Q\}$ contains simply the well recharge or discharge at the appropriate node, with recharge being positive and discharge being negative.

In the case of a confined aquifer, the solution is linear and proceeds in a time-marching manner, starting with the specified initial condition. The unconfined aquifer solution, on the other hand, is nonlinear on account of the parameter T=Kb, in which the saturated thickness b=h-B is a function of the unknown watertable head h. The solution is therefore iterative. The iterative procedure consists of substituting the calculated heads back into the equation and resolving the system. The iteration usually converges rapidly, provided the change in the saturated thickness is small relative to the thickness itself. If the change during a time step is large, or if dewatering is imminent, numerical problems can occur. The usual remedy is to reduce the time step. Special techniques must be incorporated if dewatering occurs.

A groundwater system consisting of several aquifers separated by aquitards can be represented by coupling areal models together. A multi-aquifer model of this type has been developed by Rudolph and Sudicky (1990).

5.5 Potential/Streamfunction Equations

The governing equations in a cross-sectional flow system in terms of potentials and streamfunctions are given in Section 2.4. The basic assumption is that flow is entirely within the plane of the section. Since the flow system is taken to be at steady state, the equations have no storage term. However, changes in the flow system in time, for example due to changing recharge, can be accommodated by means of successive instantaneous steady states. Although this approach neglects the storage mechanism of the system, the equilibrium solution is fully valid.

We will assume that the coordinate axes coincide with the principal directions of hydraulic conductivity. The finite element equations for the potentials and streamfunctions are:

$$[M^{\phi}]\{\phi\} = \{F^{\phi}\}$$

$$[M^{\psi}]\{\Psi\} = \{F^{\psi}\}$$

For a grid consisting of linear triangles, the coefficient matrices are:

$$[M^{\phi}]^e = \frac{K_{xx}}{4\Delta}\begin{bmatrix} b_1b_1 & b_1b_2 & b_1b_3 \\ b_2b_1 & b_2b_2 & b_2b_3 \\ b_3b_1 & b_3b_2 & b_3b_3 \end{bmatrix} + \frac{K_{yy}}{4\Delta}\begin{bmatrix} c_1c_1 & c_1c_2 & c_1c_3 \\ c_2c_1 & c_2c_2 & c_2c_3 \\ c_3c_1 & c_3c_2 & c_3c_3 \end{bmatrix}$$

$$[M^{\psi}]^e = \frac{1}{4\Delta K_{yy}}\begin{bmatrix} b_1b_1 & b_1b_2 & b_1b_3 \\ b_2b_1 & b_2b_2 & b_2b_3 \\ b_3b_1 & b_3b_2 & b_3b_3 \end{bmatrix} + \frac{1}{4\Delta K_{xx}}\begin{bmatrix} c_1c_1 & c_1c_2 & c_1c_3 \\ c_2c_1 & c_2c_2 & c_2c_3 \\ c_3c_1 & c_3c_2 & c_3c_3 \end{bmatrix}$$

$$\{F^{\phi}\}^e = q_n \frac{L^e}{2}\begin{Bmatrix} 1 \\ 1 \end{Bmatrix}$$

$$\{F^{\psi}\}^{e} = \frac{-\Delta\phi^{e}}{2}\begin{Bmatrix}1\\1\end{Bmatrix}$$

where L^e is the length of the element on the boundary, and $-\Delta\phi = \phi^i - \phi_{i+1}$ is the head change over the element having nodes i and i+1 on the boundary (Fig. 23). Upon assembly, the nodal values F_i^{ϕ} express the equivalent nodal recharge at the second-type potential boundary, which is the boundary flux multiplied by one-half the element length on either side of node i (Fig. 22). Likewise, the assembled nodal values F_i^{ψ} express one-half the negative head difference between the neighbouring nodes on either side of node i, or $(\phi_{i-1} - \phi_{i+1})/2$ (Fig. 23).

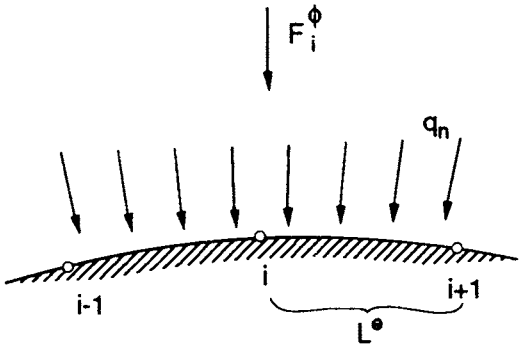

Figure 22: Second-type boundary condition for potential

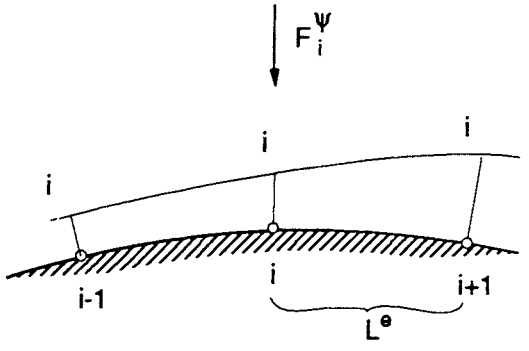

Figure 23: Section-type boundary condition for streamfunctions

First-type boundary conditions on either ϕ or ψ are accounted for in the finite element equations by partitioning the equations and moving the linking terms to the right-hand side. Thus the final coefficient matrix will contain only terms corresponding to nodes where the basic variable is unknown.

The potential/streamfunction equations can also be solved for the case where the position of the watertable (the upper boundary of the grid) is unknown. The boundary condition on ϕ will in that case be defined in terms of the recharge flux at the watertable. The condition to be satisfied is that at the watertable, the hydraulic head must equal the elevation head:

$$\phi_w = y_w$$

since the pressure component of the hydraulic head is taken to be relative to atmospheric pressure. The solution procedure for the nonlinear case starts with an assumed watertable position. The calculated head at the watertable is then compared with the elevation head, and the watertable is adjusted (up or down) accordingly. The solution is repeated until

convergence is obtained. The iterations usually converge rapidly, provided the aquifer near the watertable contains no major discontinuities.

After solution of the matrix equations for potentials and streamfunctions, the velocities can be calculated either from the potentials (see Section 4.2) or from the streamfunctions (see Section 2.4). In the latter case, we can make use of the fact that the interval in the values of the streamfunctions that bound a streamtube equals the discharge in the streamtube. Therefore, the groundwater velocity in the direction of a streamline is given by:

$$v_s = \frac{q_s}{\theta} = \frac{\Delta\psi}{\theta\Delta p}$$

where $\Delta\psi$ is the streamfunction interval, and Δp is the width of the corresponding streamtube. Since both the streamfunction and the streamtube width are continuous functions, the velocity calculated by the above procedure will be continuous between elements.

Figure 24 shows a typical finite element grid for a cross-sectional flow system. The boundary condition at the watertable is a uniform recharge of 15 cm/year, the left and bottom boundaries are impermeable, and the right boundary is an outflow boundary. The material is isotropic. The simulation starts with an initially rectangular grid, and the watertable is iteratively adjusted until a gradient that is consistent with the given recharge is obtained.

The flownet produced by the potential/streamfunction model is shown in Fig. 25 (note the vertical scale exaggeration). In (a), a uniform hydraulic conductivity of 10^{-6} m/sec is used, while in (b), the same system is modified by placement of a lens of 10^{-4} m/sec in the middle of the flow system. The high-conductive lens is seen to be highly effective in focusing the flowlines. In addition, it also reduces the watertable gradient above the lens, as well as the total watertable rise, which is 2.2 m for case (a) and 1.7 m for case (b).

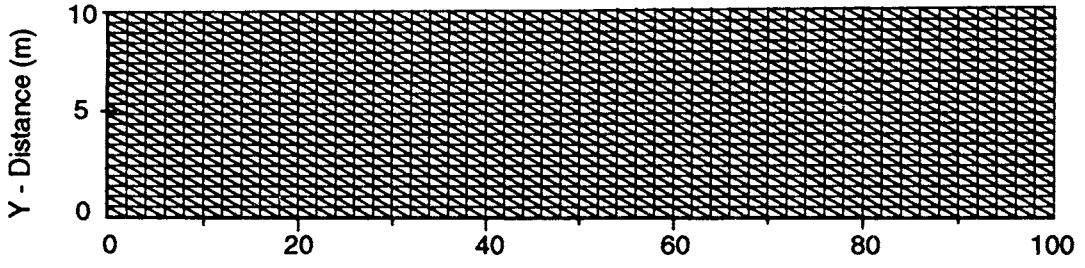

Figure 24: Finite element grid for cross-sectional flow system

5.6 Transport Equation

The governing equation for advective-dispersive transport with linear sorption and first-order decay is given in Section 2.5. The equation is valid in one, two, and three dimensions. The velocity field required for solution of the transport equation can be determined either by application of the general Darcy equation to the flow solution (see Sections 2.1 and 4.2), or by direct use of a streamfunction solution (see Section 4.5 above). The former approach is valid for both cartesian and principal coordinates, while the latter approach is used only when the transport equation is formulated in principal coordinates.

With either approach, the velocities will be element-wise constant and therefore discontinuous between elements. In the finite element solution of the transport equation,

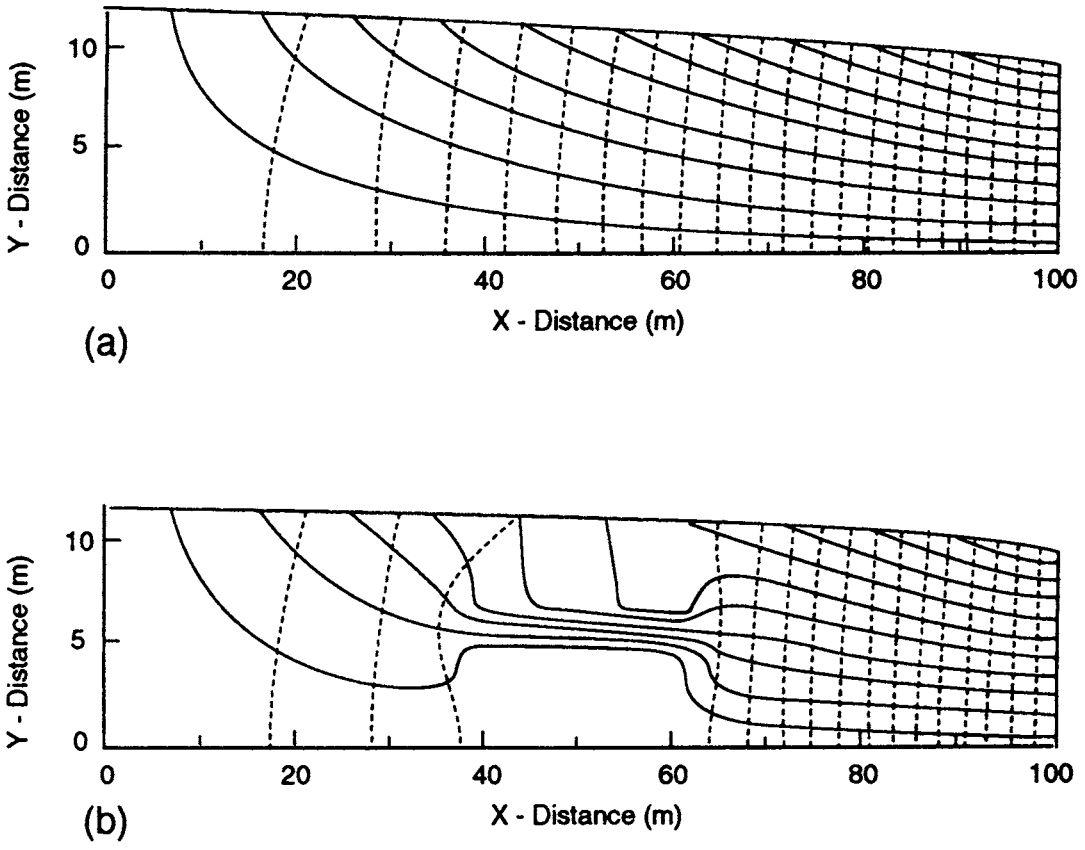

Figure 25: Flownet for cross-sectional flow system: (a) uniform material, $K=10^{-6}$ m/sec, (b) same material, except lens of $K=10^{-4}$ m/sec at center of system

this discontinuity is acceptable since the elemental parameters are integrated over the elements and the error due to the discontinuity is thereby minimized. In other approaches for the

solution of the transport equation, such as particle tracking, the discontinuity in the velocity field may not be acceptable.

We will here focus on two spatial dimensions and we will base the finite element solution on a general cartesian formulation which does not require coincidence between the coordinate axes and the principal directions. Since the numerical solution of the transport equation is sensitive with respect to time weighting, we use a general time-weighted approximation. In the absence of other information, however, a centred time weighting scheme usually gives the best accuracy in transport simulations. The finite element equation is:

$$\left\{\eta[M] + \frac{1}{\Delta t}[M^T]\right\}\{c\}_{k+1} = \left\{-(1-\eta)[M] + \frac{1}{\Delta t}[M^T]\right\}\{c\}_k + \{F^B\}$$

where η is the time weighting factor. The coefficient matrix [M] is made up of contributions as follows:

$$[M] = [M^D] + [M^V] + [M^\lambda] + [M^B]$$

where the matrices making up [M] are the dispersion, advection, decay, and boundary matrices, respectively, $[M^T]$ is the mass storage matrix, and $\{F^B\}$ is the mass flux boundary term. Both $[M^B]$ and $\{F^B\}$ arise from the third-type boundary condition. The elemental contributions to the above matrices, for linear triangles in a 2D domain, are as follows:

$$[M^D]^e = \frac{D_{xx}}{4\Delta}\begin{bmatrix} b_1b_1 & b_1b_2 & b_1b_3 \\ b_2b_1 & b_2b_2 & b_2b_3 \\ b_3b_1 & b_3b_2 & b_3b_3 \end{bmatrix} + \frac{D_{xy}}{4\Delta}\begin{bmatrix} b_1c_1 & b_1c_2 & b_1c_3 \\ b_2c_1 & b_2c_2 & b_2c_3 \\ b_3c_1 & b_3c_2 & b_3c_3 \end{bmatrix}$$

$$+ \frac{D_{yx}}{4\Delta}\begin{bmatrix} c_1b_1 & c_1b_2 & c_1b_3 \\ c_1b_1 & c_2b_2 & c_2b_3 \\ c_3b_1 & c_3b_2 & c_3b_3 \end{bmatrix} + \frac{D_{yy}}{4\Delta}\begin{bmatrix} c_1c_1 & c_1c_2 & c_1c_3 \\ c_2c_1 & c_2c_2 & c_2c_3 \\ c_3c_1 & c_3c_2 & c_3c_3 \end{bmatrix}$$

where D_{ij} are the components of the dispersion tensor, v_i are the velocity components, R is the

$$[M^V]^e = \frac{v_x}{6}\begin{bmatrix} b_1 & b_2 & b_3 \\ b_1 & b_2 & b_3 \\ b_1 & b_2 & b_3 \end{bmatrix} + \frac{v_y}{6}\begin{bmatrix} c_1 & c_2 & c_3 \\ c_1 & c_2 & c_3 \\ c_1 & c_2 & c_3 \end{bmatrix}$$

$$[M^\lambda]^e = \frac{R\lambda\Delta}{12}\begin{bmatrix} 2 & 1 & 1 \\ 1 & 2 & 1 \\ 1 & 1 & 2 \end{bmatrix}$$

$$[M^B]^e = \frac{L^e}{6}(v_x l_x + v_y l_y)\begin{bmatrix} 2 & 1 \\ 1 & 2 \end{bmatrix}$$

$$[M^T]^e = \frac{R\Delta}{12}\begin{bmatrix} 2 & 1 & 1 \\ 1 & 2 & 1 \\ 1 & 1 & 2 \end{bmatrix}$$

$$\{F^B\}^e = \frac{q_0 c_0}{\theta}\frac{L^e}{2}\begin{Bmatrix} 1 \\ 1 \end{Bmatrix}$$

retardation coefficient, q_0 is the recharge flux, c_0 is the solute concentration in the recharge flux, L^e is the length of the element side on the boundary, and l_x, l_y are the direction cosines of the inward normal at the boundary.

The above form of the mass storage matrix $[M^T]$ is known as the *consistent* form because the finite element interpolation is applied consistently to each term of the governing equation including the time derivative term. As an alternative, the *lumped* form can be obtained by adding the terms in each row of $[M^T]$ and placing the value on the diagonal. In each case, the sum of all the matrix terms must equal the total volume of the element. The consistent form gives slightly better accuracy in most applications, while the lumped form gives better convergence in some highly nonlinear problems.

A further contribution to the matrix equation is derived from the free exit boundary condition (Frind, 1988) which should be used whenever a contaminant plume reaches a domain boundary. This boundary condition does not require any known boundary values. The incorporation of the free exit boundary effectively moves the downstream boundary to infinity.

In contrast to the flow equation, the transport equation leads to an unsymmetric finite element matrix equation on account of the advective component. Standard transport models, therefore, use mostly the Gauss technique for the solution of the matrix equations. Alternatively, a special technique (Leismann and Frind, 1989) can be applied to make the transport matrix symmetrical; this facilitates solution by a highly efficient symmetrical conjugate gradient technique (Schmid and Braess, 1988).

The numerical solution of the transport equation proceeds in a stepwise manner starting with the given initial condition. If the flow system is at steady state, the flow solution is executed only once; if the flow system is transient, the flow solution must be coupled to the transport solution and executed at each time step.

Various nonlinearities can occur in the solution of the transport equation. For example, in the case of biological decay where the process depends on the availability of the reactants, the decay coefficient will be a function of the concentration of the various constituents. The mobile constituents will be represented by individual transport equations, while the immobile ones will be represented by appropriate mass balance relationships. During each time step, the solution procedure will iterate over all the transport equations while adjusting the decay coefficients until convergence occurs.

5.7 Numerical Dispersion and Numerical Constraints

Numerical dispersion is a term used to describe the numerical error that can arise in the solution of the transport equation. Its main cause is the presence of the advective term in the equation. Numerical dispersion can take the form of a smeared concentration profile, or it can cause oscillations of the profile resulting in negative concentrations or concentrations exceeding the source concentration.

In nonreactive transport, a moderate amount of numerical dispersion may be acceptable. In reactive transport, however, reactions taking place at some point in the aquifer depend on the concentration of the individual reactants at that point. Numerical inaccuracies can have profound effects on the results, as well as on the overall validity of the simulation. The control of numerical dispersion is therefore particularly vital in the simulation of reactive transport. Constraints on the numerical parameters that control numerical dispersion have been developed (Daus *et al.*, 1985).

Numerical dispersion is controlled by three factors: the spatial discretization, the time step, and the choice of the time weighting. The spatial discretization is constrained by the grid Peclet number criterion which is:

$$Pe = \frac{|\, v \,|\, \Delta L}{|\, D \,|} \leq 2$$

where $|v| = |q|/\theta$ is the magnitude of the velocity vector, $|D|$ is the effective dispersion coefficient in the direction of the velocity vector, and ΔL is the length of the element in the direction of flow. Letting $|D| = \alpha_L |v|$, the above relationship yields the constraint:

$$\Delta L \leq 2\alpha_L$$

which controls the grid spacing in the flow direction.

In practical situations, the requirement $P_e \leq 2$ cannot be easily satisfied everywhere. Fortunately, the solution is quite robust so that the occasional element exceeding the constraint (up to, say, Pe $\leq$ 4) will rarely cause difficulties. The Peclet criterion should, however, be satisfied on the average over the grid as a whole. In the direction transverse to the flow vector, the grid spacing is usually guided by the source configuration and by the expected transverse spreading behaviour, that is, a small transverse grid spacing should be chosen when the transverse dispersivity is small.

The time step is constrained by the grid Courant criterion, which is:

$$Cr = \frac{|\, v \,|\, \Delta t}{R\Delta L} \leq \frac{Pe}{2}$$

Letting Pe = 2, the time step Δt becomes:

$$\Delta t \leq \frac{R\Delta L}{|\, v \,|}$$

which physically means that a particle migrating at velocity |v| must not travel farther during one time step than the length of one element. This constraint should be satisfied for each element in the grid.

With respect to time weighting, the Taylor series expansion reveals that a centred scheme gives a higher accuracy (second-order) than either an explicit or an implicit scheme. Weighting more toward the implicit side will generally tend to dampen any oscillations that may be present, at the expense of additional smearing. Since this additional smearing has the appearance of physical dispersion due to a larger dispersivity, the results may be misleading and the use of implicit time weighting in solving the transport equation is therefore not

recommended. Overall, it has been found that reliable accuracy with essentially no numerical dispersion is obtained with a centred time weighting scheme and with the spatial and temporal discretization chosen in accordance with the grid Peclet and Courant constraints.

A further constraint on the time step arises on account of the mass loss due to decay (Luckner and Schestakow, 1986). This constraint is:

$$\Delta t \leq \frac{1}{\lambda}$$

which expresses the fact that the mass lost from any one element during a time step cannot be greater than the mass present in the element at the beginning of the time step. Exceeding this constraint will lead to negative concentrations, which, in the case of reactive systems, would cause the process to break down. Therefore this constraint must be rigorously observed.

Some of the numerical characteristics discussed above are illustrated in Figures 26, 27, and 28, which depict the solution of the 1D advection-dispersion equation under various conditions. The physical parameters are v=0.167 m/day and α=1.0 m. The boundary condition at the left is either of the first type with c/c_0=1.0 or the third type with q_0c_0/θ=0.167 m/day. The analytical solution for the first-type boundary condition, also known as the *Ogata-Banks* solution (Bear, 1979) is:

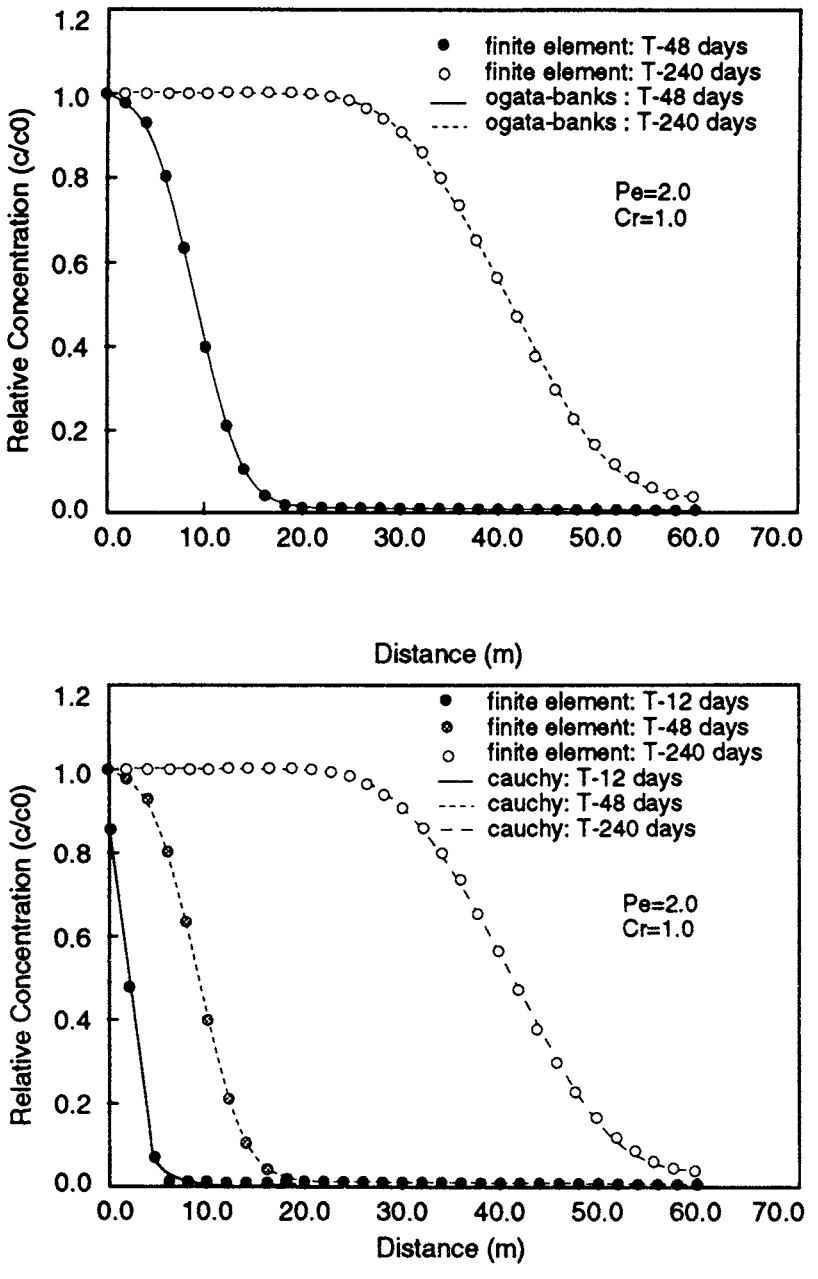

Figure 26: 1D advection-dispersion solution, numerical vs. analytical

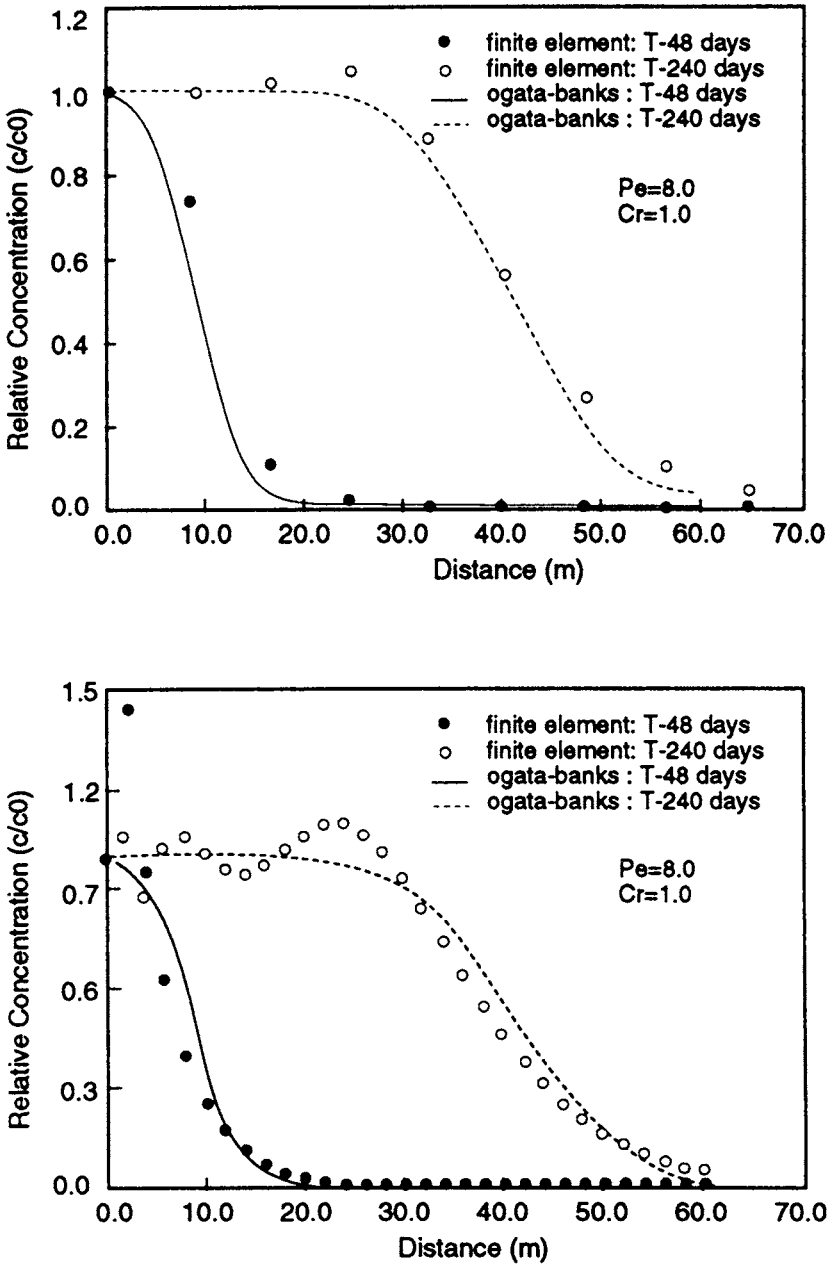

Figure 27: 1D advection-dispersion solution, numerical vs. analytical

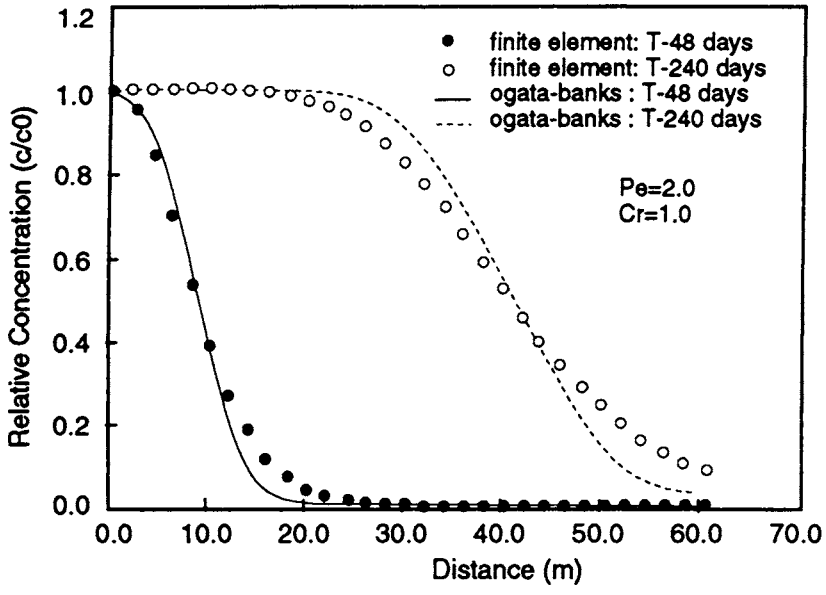

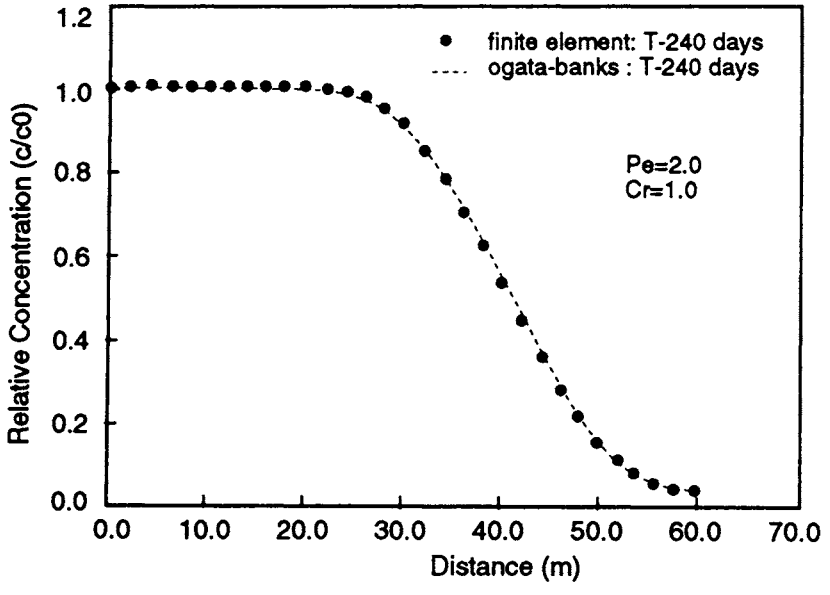

Figure 28: 1D advection-dispersion solution, numerical vs. analytical

$$\frac{c(x,t)}{c_0} = \frac{1}{2}\left[erfc\left\{\frac{x-vt}{2\sqrt{Dt}}\right\} + \exp\left\{\frac{vx}{D}\right\} erfc\left\{\frac{x+vt}{2\sqrt{Dt}}\right\}\right]$$

where the complementary error function erfc{.} is defined as:

$$erfc(u) = \frac{2}{\sqrt{\pi}} \int_u^\infty e^{-\xi^2} d\xi$$

The first term in the above solution gives the symmetric advection-dispersion profile, while the second term gives the effect of the first-type boundary which becomes smaller with increasing distance from the boundary.

The corresponding solution for the third-type boundary condition (Bear, 1979) is:

$$\frac{c(x,t)}{c_0} = \frac{1}{2}\left[erfc\left\{\frac{x-vt}{2\sqrt{Dt}}\right\} - \exp\left\{\frac{vx}{D}\right\} erfc\left\{\frac{x+vt}{2\sqrt{Dt}}\right\}\left\{1+\frac{vx+v^2t}{D}\right\}\right] + \frac{v\sqrt{t}}{\sqrt{\pi D}} \exp\left\{-\frac{(x-vt)^2}{4Dt}\right\}$$

Figure 26 is a comparison of the two types of boundary conditions. With the first-type boundary, the solution starts immediately at c/c_0=1.0, while with the third-type boundary, it starts at c/c_0=0 and gradually builds up to c/c_0=1.0. As a result, the mass input is greater during the early time period for the first-type boundary case, which has a constant mass input. Also the point where c/c_0=0.5 coincides with the point x=vt in the third-type boundary case, but is slightly ahead in the first-type boundary case. The two profiles approach each other with increasing time. Since the recommended spatial and temporal discretization is used and the time weighting is centred, the numerical solution closely agrees with the analytical solution

in both cases.

Figure 27 shows the effect of exceeding the discretization constraints. In Figure 27a, the grid spacing is four times the recommended value according to the Peclet constraint, the result is significant overshoot and smearing of the profile. In Figure 27b, the time step exceeds the value recommended by the Courant constraint by a factor of four; this also generates fairly large oscillations.

In Fig. 28a, an implicit (backward) time-weighting is used instead of a centred time weighting. This causes a marked smearing of the profile (compare with Fig. 26a). Figure 28b shows the effect of using a lumped mass storage matrix; the accuracy obtained with this formulation is comparable to that obtained with the consistent mass matrix (compare again with Fig. 26a).

5.8 Case Studies

There are numerous studies where models that are based on finite element methods have been used to predict groundwater flow and movement of contaminants in aquifers. The case study presented in Appendix 2 (Ophori and Farvolden, 1985) describes how a numerical model was used to evaluate the use of a hydraulic trap for preventing collector well contamination in the Forwell aquifer, Ontario, Canada. The source of contamination was described as an oil reclamation plant which operated over a period of approximately two decades. Contamination from the lagoons used for sludge waste disposal migrated through the aquifer, contaminating an estimated volume of 30,000 m^3 of groundwater.

The study describes extensive literature search and detailed pumping and recovery tests to characterize the aquifer. Hydraulic parameters obtained during the literature search and field tests were used as input into the numerical model developed to simulate groundwater flow near steady state field conditions. Triangular finite elements were used in the study, with finer mesh in the vicinity of the pumping wells. The model was calibrated by adjusting inferred

boundaries until the water levels predicted by the model were similar to observed data. The calibrated model was then used to determine the effect of a hydraulic trap in the form of a purge well which was intended to provide protection against contamination from the collector well.

Another study is presented in Appendix 3 where finite elements method was used to investigate a concept that would ordinarily be difficult to demonstrate. A 1D saturated-unsaturated flow model was applied to the transient drainage of water through a two-layer vertical column of porous media. The objective was to demonstrate the hydraulic principles involved in the use of fine-grained materials as protective covers for reactive mine tailings. The objective of installing the covers is to keep the materials at high moisture content thereby reducing the influx of oxygen into the reactive tailings. In the study provided in Appendix 3, emphasis was placed on the choice of materials which have appropriate physical properties to achieve the set objectives because of the dependence of observed response of the two-layer system on the retention characteristics of the component materials. The study further demonstrates how models could be used for the purpose of system design.

6. PARTICLE TRACKING METHODS

Particle tracking methods offer a valuable alternative to finite difference and finite element methods for simulating contaminant transport. In particle tracking, the distribution of a solute in the groundwater is represented by a finite number of particles, where each particle carried either a certain concentration or a certain fraction of the total mass. The particles are moved through the domain according to the velocity field, and their behaviour is observed. The status of the system at a given time can be deduced from the distribution of the particles. The accuracy and smoothness of the solution will depend on the number of particles used.

One of the main advantages of particle tracking is that the Peclet constraint on the grid spacing does not apply and that the type of numerical dispersion that is controlled by this